Published in final edited form as:
Toxicology. 2008 February 28; 244(2-3): 98–110. doi:10.1016/j.tox.2007.10.020.

Characterization of Chlorpyrifos Induced Apoptosis in Placental Cells

Marilyn D. Saulsbury, **Simone O. Heyliger**, **Kaiyu Wang**, and **Dorothy Round**
Department of Pharmaceutical Sciences, School of Pharmacy, Hampton University, Hampton, VA 23668

Abstract

The mechanism by which chlorpyrifos exerts its toxicity in fetal and perinatal animals has yet to be elucidated. Since the placenta is responsible for transport of nutrients and is a major supplier hormones to the fetus, exposure to xenobiotics that alter the function or viability of placenta cells could ostensibly alter the development of the fetus. In this study, JAR cells were used to determine if CPF and the metabolites 3,5,6-trichloro-2-pyridinol (TCP) and chlorpyrifos-oxon (CPO) are toxic to the placenta. Our results indicate that chlorpyrifos (CPF), and its metabolite chlorpyrifos-oxon (CPO) caused a dose-dependent reduction in cellular viability with CPF being more toxic than its metabolites. Chlorpyrifos-induced toxicity was characterized by the loss of mitochondrial potential, the appearance of nuclear condensation and fragmentation, down- regulation of Bcl-2 as well as up-regulation of TNFα and FAS mRNA. Pharmacological inhibition of FAS, nicotinic and TNF-α receptors did not attenuate CPF-induced toxicity. Atropine exhibited minimal ability to reverse toxicity. Furthermore, signal transduction inhibitors PD98059, SP600125, LY294002 and U0126 failed to attenuate toxicity; however, SB202190 (inhibitor of p38α and p38β MAPK) sensitized cells to CPF-induced toxicity. Pan-caspase inhibitor Q-VD-OPh produced a slight but significant reversal of CPF-induced toxicity indicating that the major caspase pathways are not integral to CPF-induced toxicity. Taken collectively, these results suggest that chlorpyrifos induces apoptosis in placental cells through pathways not dependent on FAS/TNF signaling, activation of caspases or inhibition of cholinesterase. In addition, our data further indicates that activation of p38 MAPK is integral to the protection cells against CPF-induced injury.

1. Introduction

Chlorpyrifos (CPF), an ogranophosphate, is currently utilized as a pesticide on more than 40 crops food crops including such as peaches, citrus, almonds and grapes. CPF and its metabolites have been detected in farm animals, such as cattle, hogs and sheep (Ivey 1979; Ivey and Palmer 1979; Ivey and Palmer 1981). Moreover, chlorpyrifos residues or its metabolites have been discovered in the diet of preschoolers (Fenske et al. 2002a), in the urine of children living in proximity to orchards (Lu et al. 2000; Fenske et al. 2002b), as well as in the cord blood of infants born to minority women living in urban settings (Whyatt et al. 2004).

The ubiquitous presence of chlorpyrifos residues and pesticide mixtures has raised concerns about the safety limits of these compounds. Although, CPF has been shown to be relatively

CORRESPONDING AUTHOR: Marilyn D. Saulsbury, Ph.D., Department of Pharmaceutical Sciences, School of Pharmacy, Hampton, VA 23668, marilyn.saulsbury@hamptonu.edu.

safe in adult animals, newly discovered evidence indicates that CPF is a developmental neurotoxicant in the fetus and is thus harmful (Garcia et al. 2003). In animals and cellular models, chlorpyrifos inhibits neural cellular replication (Qian et al. 2001), interferes with cellular differentiation (Crumpton et al. 2000), evokes oxidative stress, alters neurotransmission (Dam et al. 1999; Bloomquist et al. 2002; Karanth et al. 2006; Slotkin and Seidler, 2007) and induces neurobehavioral changes (Ricceri et al. 2006). Additionally, animals exposed to CPF *in utero* or as juveniles display motor and cognitive delays (Moser 2000). In humans, elevated levels of chlorpyrifos in umbilical cord plasma are inversely associated with birth weight and length in children born to minority women (Whyatt et al. 2004). The literature indicates that chronic CPF exposure is associated with decreased birth weight and length. In addition, lower birth weights have specifically been documented among African Americans infants (Rauh et al. 2006; Perera et al. 2003) exposed to *CPF in utero*. Finally CPF exposure is associated with alterations in developmental and psychomotor indices in Mexican-American children (Eskenazi, et al. 2007) and with immunological abnormalities (Thrasher et al 2002). Consequently, chlorpyrifos is ranked 125 on 2001 CERCLA List and the United States Environmental Protection Agency (USEPA) has placed restrictive guidelines on its utilization specifically inside the home; however, despite these restrictions CPF still lingers in many dwellings (Whyatt et al. 2007).

Despite the mounting evidence that CPF can be harmful to children and the developing fetus, the mechanism(s) of action have yet to be fully elucidated. Although most studies have focused on the direct effect of CPF on the fetus, very few have assessed the effect of CPF on the placenta. This is disconcerting due to the fact that the placenta is a major supplier of nutrients, cytokines and hormones, which regulate implantation and fetal maturation. In addition, the placenta has been shown to serve as a *de facto* liver for the fetus and is capable of detoxifying xenobiotics through the actions of phase 1 and phase 2 metabolizing enzymes such as cytochrome P_{450} isoenzymes, N-acetyltransferase, and UDP-glucuronosyl transferase. Hence, the placenta represents a possible model for predicting the effects of overall fetal development and viability once exposed to a xenobiotic.

Recent literature indicates that low-level exposure to environmental contaminants may indeed interfere with placental function (Myllynen et al. 2005; Mose et al. 2006; Sagiv et al. 2007). For example, endosulfan inhibits aromatase activity; whereas, methomyl, pirimicarb, propamocarb, iprodion, lindane and bisphenol-A enhance placental aromatase activity (Nativelle-Serpentini et al. 2003). TCDD exposure is associated with fetus loss and the alteration of the secretion of chorionic gonadotropin hormone in primates (Guo et al. 1999; Chen et al. 2003; Myllynen et al. 2005). With regards to chlorpyrifos, CPF and/or its metabolites have been detected in the fetuses of dams administered CPF perinatally (Mattsson et al. 2000; Abdel-Rahman et al. 2002). Abdel-Rahman and colleagues (2002) further concluded that though the placenta presents a barrier of protection against CPF; at high doses, CPF and its metabolites can cross the placenta and enter into the fetus despite extensive maternal hepatic metabolism, as well as, distribute to all fetal tissues and plasma with elimination occurring at a slow rate. In addition, Souza et al. (2004) demonstrated that CPF alters the enzymatic activity of placental PI4-kin ase and phosphatidylinositol handling suggesting that CPF may have membrane disrupting properties. Given that exposure to xenobiotics can alter the function and viability of placenta cells, thereby ostensibly, altering the growth and development of the fetus, we examined whether chlorpyrifos and its metabolites are toxic to placental cells.

2. Materials and methods

2.1. Reagents

FAS/FASL antagonist, LY294002, QVDOPh, PD98059, TNF-α antagonist (WP9QY) and U0126 were obtained from Calbiochem (San Diego, CA, USA). Chlorpyrifos and its metabolites Chlorpyrifos-oxon and 3,5,6-trichloro-2-pyridinol were purchased from ChemService (West Chester, PA, USA). Alamar Blue was obtained from Serotec and the Human Stress PCR Array was obtained from SuperArray (Frederick, MD, USA). Unless otherwise stated, all other reagents were purchased from the Sigma Chemical Company (St. Louis, MO, USA).

2.2. Cell Culture

Human placental choriocarcinoma (JAR) cells were purchased from ATCC and propagated in RPMI-1640 supplemented with penicillin (100U/ml), streptomycin (100mM) and 10% v/v fetal bovine serum.

2.3. Cytotoxicity Studies

Chlorpyrifos and its metabolites were purchased from ChemService and used within days of purchase. Chlorpyrifos and metabolites were initially dissolved in DMSO at stock concentrations of 100mM. CPF was diluted with media so that DMSO concentrations did not exceed a final concentration of 0.01% v/v. Viability studies were conducted utilizing JAR cells plated in 48 well plates at a density of 10,000 cells per well in RPMI-1640 supplemented with penicillin (100U/ml), streptomycin (100mM) and 10% FBS. On the day of the experiment(s) the cells were incubated with various concentrations of chlorpyrifos (CPF) and its metabolites chlorpyrifos-oxon (CPO) and 3,5,6-trichloro-2-pyridinol (TCP) for 24 hours in the presence of serum free media (RPMI-1640 supplemented with penicillin (100U/ml), streptomycin (100mM) and 0.1% Bovine Serum Albumin). Serum supplementation was replaced with 0.1% BSA because our laboratory has previously observed that serum content (10% or greater) reduces efficacy of chlorpyrifos. This observation was further corroborated by Qiao et al. 2001. In addition our laboratory has observed that exposure to serum free media supplemented with 0.1% does not alter cellular viability during the experimental time points.

Inhibitory studies were conducted by incubating cells with 60μM CPF in the presence and absence of 30μM PD98059 (ERK inhibitor), 10μM U0126 (MEK inhibitor), 10μM SB202190 (p38 MAPK inhibitor), 10μM SP600125 (JNK inhibitor), 20μM LY294002 (PI3K inhibitor), 50μM QVDOPh (Pan-Caspase Inhibitor), 1mg/mL FAS/FASL antagonist, 10μM Atropine (muscarinic cholinergic receptor antagonist) and 100μM TNF-α antagonist for 12 or 24 hours. All inhibitors except FAS/FASL antagonist and Mecamylamine were dissolved in DMSO at concentrations of 10mM. FAS/FASL antagonist was dissolved directly into media; whereas, stock solutions of Mecamylamine were prepared at concentrations of 100mM. In inhibitor studies, DMSO concentrations did not exceed 0.05% v/v. After the incubation period, fresh media containing 10% Alamar Blue (v/v) was added and cells were incubated for 8 hours at 37°C in an atmosphere of 5% CO_2. Cytotoxicity produced in the Alamar Blue assay was also confirmed using the crystal violet viability assay. The microplates were read at 570nm with reference wavelength 630 nm using a BioRad Benchmark Plus Microplate Reader.

2.4. Assessment of Mitochondrial Potential

Cells will be seeded in 12-well plates at a density of 10,000 cells per well. Cells were treated with 60μM CPF for 24 hours. Ten minutes prior to the end of the incubation period, cells will be loaded with 15μM JC-1 (5,5′,6,6′-tetrachloro-1,1′,3,3′-tetraethyl-. benzimidazolylcarbocyanine Iodide) dye (in RPMI-1640 without phenol red) for 10 minutes

at 37°C. The cells were washed with Dulbecco's phosphate buffered saline (DPBS) and then fresh media was added to the wells. Cells were then immediately examined using a Nikon inverted phase contrast epifluorescent microscope equipped with a triple cube filter for the simultaneous detection of rhodamine, FITC and DAPI.

2.5. Morphological Studies

Nuclear morphology was assessed using Hoechst 33342 stain. Cells were grown in 48 well plates (10,000 cells per well) and then treated with 60μM CPF for 24 hours. Following incubation period, the media was removed and cells were incubated in phenol red-free RPMI containing 50μM of Hoechst stain for sixty (60) minutes at 37°C in an atmosphere of 5% CO_2. The cells then were rinsed with Hanks Balanced Salt Solution and nuclear morphology was immediately analyzed using a Nikon inverted phase contrast epifluorescent microscope equipped with a triple cube filter for the simultaneous detection of rhodamine, FITC and DAPI.

2.6. Caspase 3/7 Assay

The Caspase-Glo® 3/7 Assay (Promega, WI) was performed according to the manufacturer's specifications. In short, JAR cells were seeded in ninety-six (96) well plates at 20,000 cells per well and allowed to acclimate overnight. On the day of the experiment, the cells were switched to phenol red-free RPMI supplemented with 0.1% BSA. CPF was added at a final volume of 100μL/well at the following concentrations: 600, 300, 150, 75, 37.5 and18.75 μM. Controls wells were treated with drug vehicle with equivalent volumes of DMSO as the CPF treated wells. Staurosporine (10μM) was used as a positive control and indicator of caspase activation. Cells were incubated with various concentrations of CPF or 10μM staurosporine in the presence and absence of Pan-Caspase inhibitor 50μM Q-VD-OPh ((N-(2-quinolyl)valyl-aspartyl-(2,6-difluorophenoxy)methylketone)) for four (4) hours. Following the incubation, 100μL of Caspase-Glo was added to each well and the plates were for one (1) hour at 37°C. The admixtures (CPF and Caspase-Glo) were transferred to a white opaque ninety-six (96) well plates and read using a Thermal Electron Luminoskan luminometer. Data was expressed as percent change over control.

2.7. Real-Time PCR Array

JAR cells were treated with of 60μM CPF for 24 hours. Total RNA was extracted utilizing the QIAGEN RNAeasy kit according to manufacturer's instructions. Total RNA was then treated with DNAse I (according to manufacturer's instructions) to remove genomic DNA. cDNA was synthesized utilizing the BioRad iScript cDNA synthesis kit and subjected to SuperArray Human Stress and Toxicity Real –Time PCR array analysis according to manufacturer's instructions.

2.8. Statistics

The one-way ANOVA test with Tukey post-hoc analysis was employed to calculate the statistical significance between control and treated groups. A p-value < 0.05 was considered to be statistically significant. The IC_{50} values were calculated using GRAPHPAD PRISM software whereby dose response curves generated from JAR cells exposed to chlorpyrifos or its metabolites for 24 hours were fitted to the following equation: Y=Bottom+ (Top-Bottom)/(1+10^((LogEC_{50}-X))).

3. Results

3.1. Chlorpyrifos Induces Apoptosis in JAR Choriocarcinoma Cells

Chlorpyrifos (CPF) and chlopyrifos-oxon (CPO) caused dose dependent reductions in JAR viability at concentrations greater 15μM as early as 24 hrs post-exposure (Figures 1 and 2) and

extended to at least 72 hours. The IC_{50} values at 24 hrs for CPF and CPO were 59.1 ±1.19 μM and 147±1.926 μM, respectively. TCP was the least toxic of the compounds tested with an IC_{50} of greater than 250μM. Since CPF was the most toxic species, further characterization of pesticide toxicity was performed using only CPF. For ease of dilution, 60 uM was used as the IC_{50} concentration for CPF when conducting our toxicity experiments. Chlorpyrifos toxicity was accompanied by mitochondrial damage as evidence by nuclear condensation and fragmentation (Figure 4) and by the loss of mitochondrial potential (Figure 5). The loss of mitochondrial potential coupled with nuclear condensation and fragmentation indicates the presence of apoptosis.

To determine if caspases mediate CPF-induced toxicity, Caspase 3/7 activity was measured in CPF-treated cells for four (4) hours (Figures 6A). In parallel studies, JAR cells were also incubated with 10μM Staurosporine, an established activator of caspase enzymes and a known inducer of apoptosis. Concentrations of CPF that were greater than 150μM caused significant increases in caspase 3/7 activity relative to vehicle control ($p<0.001$). Staurosporine caused 182% increase in caspase 3 activity (Table 1). Pretreatment with Q-VD-OPh, a broad spectrum inhibitor of caspase 3, 9, 8, 10 and 12-mediated apoptosis (Caserta et al. 2003) totally reversed staurosporine (Table 1) and CPF-induced activation of caspase 3/7 (Figure 6A).

To determine if Q-VD-OPh inhibition of caspase activation will attenuate CPF-induced cellular death, cells were pretreated with 50μM Q-VD-OPh (N-(2-quinolyl)valyl-aspartyl-(2,6-difluorophenoxy)methylketone. Q-VD-OPh produced a slight but significant ($p<0.05$) reversal of CPF-induced toxicity indicating that the major caspase pathways caspase 3/9, caspase 8/10 and caspase 12 may not be integral to CPF-induced toxicity. It should be noted that Q-VD-OPh does not inhibit calpains (Yang et al. 2004) and thus CPF-induced toxicity may be mediated via the activation of these serine proteases or other proteolytic processes.

3.2. Atropine Partially Reverses Chlorpyrifos-Induced Toxicity in JAR cells

On the basis of our experiments, caspases seemingly do not play a major role in mediating CPF toxicity, therefore the possible role of cholinergic activation in CPF-induced apoptosis was further examined. CPF like most organophosphates derive their killing effects in insects as well as their side effects in mammals by inhibiting cholinesterase. Once acetylcholinesterase and pseudocholinesterases are inactivated, acetylcholine accumulates leading to cholinergic hyperactivity in tissues which express muscarinic and/or nicotinic receptors. Since the placenta has a functional cholinergic system complete with cholinergic receptors, choline acetyltransferase (ChAT) and cholinesterase, it is feasible that CPF-induced toxicity is caused, in part, by cholinergic hyperactivity in the placenta. JAR cells were exposed to chlorpyrifos in the presence and absence of either muscarinic receptor antagonist atropine or the nicotinic receptor antagonist mecamylamine (Figures 7A and 7B). Atropine (10μM) offered slight but significant protection against the toxic effects of chlorpyrifos; however, mecamylamine (100μM) failed to attenuate the CPF-induced toxicity. Our data suggests that stimulation of muscarinic receptors may contribute to CPF-induced toxicity.

3.3. Inhibition of p38 MAP Kinase Sensitizes JAR Cells to Chlorpyrifos

To ascertain which signal transduction pathway mediated the toxic effects of CPF, JAR cells were exposed to chlorpyrifos in the presence and absence of several inhibitors 30μM PD98059, 10μM U0126, 10μM SB202190, 20μM LY294002 for 12 and 24 hours. None of the signal transduction inhibitors reversed the toxic effects of CPF at 24 hours (data not shown). Thus whether these signal transduction inhibitors accelerated or delayed CPF-induced toxicity at 12 hours was assessed. At 12 hours, CPF is only slightly toxic. Significant toxicity (less than at 60% viability) is observed at a concentration of 60μM between 20–24 hours post exposure. PD98059, U0126, SB202190 and LY294002 failed to alter the toxic effects of CPF (figures

8A–D). Cells exposed to SP100625, U0126 and LY294002 exhibited slight but significantly enhanced cellular toxicity. The addition of CPF to these cells enhanced toxicity; however, these effects constitute an additive effect rather than potentiation. Conversely, administration of 10μM SB202190 had little effect on cellular viability; however, the addition of SB202190, a potent and selective inhibitor of p38 MAPK, to CPF-treated cells accelerated and potentiated CPF-induced toxicity (Figures 9A and B) Hence our results indicate that p38 MAPK mediates pathways which may protect cells from injury associated with exposure to CPF.

3.4. Chlorpyrifos Toxicity is Associated with Up-Regulation of FAS and TNF-α mRNA but not dependent on activation of FAS and TNF-α

To further characterize CPF-induced toxicity, the effects of CPF on pro-apoptotic gene expression was investigated. Of the approximately 80 genes tested four (4) genes were up-regulated including Tumor Necrosis Factor-alpha (TNF-α), FAS, ITGA4 and ITGB1. TNF-α and FAS experienced the greatest fold change at 11.84 and 15.89 respectively. Conversely, five (5) genes were significantly reduced relative to the control. These included Bcl-2, Cyclin-dependent kinase inhibitor 2A (CDKN2A), metastasis associated 1 family member 2 (MTA2), TWIST and TEK (Table 1). Since FAS and TNF-α are pro-apoptotic mediators, we decided to determine if activation of these genes mediated CPF induced apoptosis. CPF treated cells were exposed to pharmacological inhibitors of TNF receptor and FAS (figures 10A and B). Neither TNF receptor nor FAS antagonist reversed CPF-induced toxicity; however, inhibition of TNF caused a slight but significant potentiation of CPF-induced toxicity. These results indicate that FAS and TNF probably do not play a pivotal role in mediating CPF toxicity but suggest that TNF expression may protect the cell from injury upon exposure to CPF.

4. Discussion

Our studies examined the effects of chlorpyrifos on placenta viability and gene expression. Our findings indicate that chlorpyrifos and its metabolites, chlorpyrifos-oxon (CPO) and 3,5,6-trichloro-2-pyridinol (TCP), produced dose-dependent reductions in cellular viability (Figures 1–3). CPF induced toxicity at concentrations as low as 15μM whereas both CPO and TCP produced toxicity at slightly higher concentrations, thus indicating that toxicity in JAR cells are primarily mediated through exposure to the parent compound. This is surprising because CPO is considered to be more toxic than CPF primarily because CPO is the active species primarily responsible for inhibiting cholinesterase.

Since CPF was the most toxic species, further characterization of pesticide toxicity was performed using only CPF. The effects of CPF on nuclear morphology and mitochondrial function were examined. CPF (at 60μM) was associated with nuclear condensation and fragmentation (Figure 4). Moreover, CPF toxicity is associated with the loss of mitochondrial potential as demonstrated by a spectral shift by the JC-1 dye from red to green (Figure 5). Additionally, at higher concentrations, exposure to CPF within 4 hours leads to a dose-dependent increase of caspase3/7 activity (Figure 6A). In addition, pan-caspase inhibitor Q-VD-OPh partially attenuated CPF-induced toxicity (Figure 6B) and abrogated Saturosporine and CPF-induced activation of caspase 3/7 (Table 1, Figure 6A). It should be noted that Q-VD-OPh does not inhibit calpains (Yang et al. 2004) and thus CPF-induced toxicity may be mediated via the activation of these serine proteases or other proteolytic processes. Nonetheless, these observations are consistent with the induction of apoptosis and corroborate earlier findings which indicated that CPF induces toxicity through apoptotic mechanisms (Caughlan et al. 2004;Nakadai 2006) and only partially through activation of the caspase system (Nakadai 2006).

Because caspase inhibition yielded only limited protection against CPF, we further characterized and explored additional mechanisms which could underlie CPF-induced toxicity.

CPF like most organophosphates derive their insecticide properties as well as their deleterious effects in mammals by primarily inhibiting cholinesterase. Once acetylcholinesterase and pseudocholinesterases are inactivated, acetylcholine accumulates leading to cholinergic hyperactivity in tissues which express muscarinic and/or nicotinic receptors (for extensive review see Sastry 1997). Since the placenta has a functional cholinergic system complete with cholingeric receptors, choline acetyltransferase (ChAT) and cholinesterase, it is feasible that CPF imparts toxicity in the placenta by inducing cholinergic hyperactivity.

To explore this possibility, CPF induced toxicity was assessed in the presence and absence of cholinergic receptor antagonists, atropine and mecamylamine. Atropine, a muscarinic receptor antagonist, partially attenuated CPF-induced toxicity (figure 7A) whereas, mecamylamine, a nicotinic receptor antagonist, failed to protect cells against the toxic effects of CPF (figure 7B), thereby indicating that inhibition of cholinesterase and the subsequent activation of muscarinic receptors may be a contributing factor to CPF-induced toxicity. Indeed, muscarinic receptor activation in cardiac and neuronal tissues is associated with reactive oxygen species generation and the induction of neuronal apoptosis (Naarala et al. 1997; Li, etal. 2001; Oldenburg, et al. 2002). Moreover, several studies implicate oxidative stress as a major contributor to CPF-induced toxicity (Qiao et al. 2005; Slotkin et al. 2005; Giordano, 2007; Tuzmen et al. 2007).

To identify other pathways involved in the induction of apoptosis, the effects of select signal transduction inhibitors on CPF-induced toxicity were examined. None of the signal transduction inhibitors tested attenuated the toxic effects of CPF (data not shown) at 24 hours. At 12 hours, 60μM CPF is slightly toxic to JAR cells, however, the addition of SP100625 (JNK inhibitor), U0126 (MEK inhibitor), LY294002 (P-I3K inhibitor) and SB202190 (p38α and p38β MAPK inhibitor) significantly enhances cellular death (figures 8 and 9). It should be noted that SP100625, U0126 and LY294002 are also toxic to JAR cells and thus enhanced toxicity exhibited in the presence of CPF may constitute an additive effect.

Conversely, SB202190 is not toxic to JAR cells and the combination bolus of CPF and SB202190 led to large reduction cellular viability as seen figures 9A and 9B. This data suggests that the activation of the p38MAPK signaling pathway is necessary for protection against CPF induced toxicity. This is surprising because p38 MAPK is a stress-related MAPK which is activated via phosphorylation in response to a myriad of chemical and oxidative insults (Namgung and Xia 2000; Cai et al. 2006; Tanel and Averill-Bates 2007). Historically, sustained activation of p38MAPK is associated with apoptosis and conversely inhibition rescues cells from apoptotic death (Chang and Karin 2001; Mansouri et al. 2003; Cai et al. 2006; Zhou et al. 2006; Tanel and Averill-Bates 2007). It should be noted that SB202190 inhibits both p38α and p38β and that p38α is pro-apoptotic whereas p38β MAPK isoform may be associated with activation of pro-survival pathways (Nemoto et al. 1998). Indeed, a recent study by Caughlan et al. (2004) demonstrated that CPF activates p38 MAPK and that SB202190 accelerates CPF-induced toxicity in cortical neurons. Although this study did not identify which isoforms were activated it is possible that CPF induces toxicity by preferentially activating p38α and the subsequent inhibition of p38β by SB202190 greatly augments CPF-induced activation of p38α. Nonetheless, our findings corroborate observations made by Caughlan and her colleagues (2004). Hence our data suggest that activation of p38MAPK involvement in CPF-induced toxicity is not specific to neuronal tissues but may be integral to a variety of cell types.

To further characterize CPF toxicity, the effects of CPF on key genes known to regulate apoptosis was examined. Of the approximate eighty (80) genes tested, five (5) genes were identified that demonstrated significant down-regulation and four (4) genes were significantly up-regulated relative to the controls. The down-regulated genes included Bcl-2, CDKN2A, MTA2, TEK and TWIST1 whereas the up-regulated genes included FAS, TNF-α, ITGB1 and

ITGA4 with TNF and FAS registering the greatest up-regulation at 15.9 and 11.8 fold increases respectively. Since both FAS and TNF are well established mediators of apoptosis (Itoh et al. 1991) we decided to further investigate the possible roles in CPF-induced toxicity. FAS (CD95), a transmembrane receptor that is a member of the TNF receptor superfamily, is found in numerous immune and non-immune tissues. When bound to Fas ligand (FasL), Fas initiates a cascade of events which leads to the recruitment of the Fas-associated death domain adaptor protein (FADD) as well as pro-caspases (particularly pro-caspase 8) and culminates in the formation of death-inducing signaling complex (DISC) (Kreuz et al. 2004). The DISC ultimately activates proteolytic enzymes which systematically destroy proteins and DNA required for cellular viability and produces the hallmark signs of apoptosis including plasma membrane blebbing, nuclear condensation and loss of mitochondrial potential (for extensive reviews see Strasser et al. 2000; Houston and O'Connell 2004; Beere, 2005).

TNF-α, alternatively, is a pleiotrophic cytokine which possesses both pro-apoptotic and anti-apoptotic properties. TNF-α-induced apoptosis is mediated by the binding of TNF to the TNF receptor subtype 1 (TNFR1). This interaction leads to the recruitment of the multimeric protein complex consisting of TNFR1, TNF receptor associated death domain (TRADD), receptor interacting protein (RIP), and TNFR associated factor 2 (TRAF2) and Fas associated death domain (FADD) proteins (Chen and Goeddel 2002; Li and Minden. 2005). This protein complex, in return, recruits and activates a protease cascade that leads to apoptosis (Chen and Goeddel 2002). Activation of pro-survival pathways also requires the creation of the aforementioned multimeric protein complex as well as the subsequent activation of TAK1 and MEKK. TAK1, MEKK, TRAF2 and RIP together recruit and activate IκB kinase (IKK), which in turn phosphorylates IκB (Devin et al. 2000; Blonska et al. 2005). The phosphorylation, ubiquination and subsequent degradation of IκB enable the translocation of NFκB to the nucleus where it binds to response elements in DNA to activate cellular protective genes. Thus, the ability of TNF-α to induce apoptosis is dependent on which of the pathways predominates since abrogation of NFκB enhances apoptosis while reinforced activation of NFκB protects against apoptosis (Chen and Goeddel 2002).

To determine whether CPF-induced apoptosis is caused by the enhanced expression of TNF or FAS, JAR cells were treated with a pharmacological antagonist of TNF receptor (WP9QY) and FAS. WP9QY (YCWSQYLCY) is a cyclic peptide that structurally resembles TNF at its receptor recognition loop and binds to TNFR1, thereby preventing TNF from interacting with its receptor (Suzuki et al. 2006). Our data indicate that neither WP9QY nor FAS antagonist reversed CPF-induced apoptosis (Figure 10). TNF receptor antagonist; however, did produce a slight but significant augmentation of the toxic effects of CPF. Overall, our data suggest that TNF and FAS may not participate directly in CPF toxicity; however, our data does suggest that elevation of TNFα may protect the cells against CPF effects. It should be noted that a recent study indicated that FAS may not be active in some placental tissues. The authors further concluded that FAS may play yet an undetermined role. Nonetheless, our data corroborate earlier reports which state that TNF-α levels are elevated in animals exposed to CPF (Gordon and Rowsey, 1999; Rowsey and Gordon, 1999). Thus our findings imply that CPF can modulate TNF expression at the transcriptional level. In summary, it has been demonstrated that CPF is toxic to the placenta cells. Taken collectively, our data presents a plausible mechanism by which environmental contaminants such as chlorpyrifos (CPF) can negatively impact fetal development.

Acknowledgments

Funding for this work was provided by ATSDR- Environmental Health, Health Services and Toxicology Research Program cooperative agreement # 5 U50 TS 473408 and by the National Institutes of Health–Minority Biomedical Research Support program grant#5S06GM066093.

References

Abdel-Rahman AA, Blumenthal GM, Abou-Donia SA, Ali FA, Abdel-Monem AE, Abou-Donia MB. Pharmacokinetic profile and placental transfer of a single intravenous injection of [(14)C]chlorpyrifos in pregnant rats. Arch Toxicol 2002;76(8):452–9. [PubMed: 12185413]

Andersen HR, Vinggaard AM, Rasmussen TH, Gjermandsen IM, Bonefeld-Jørgensen EC. Effects of currently used pesticides in assays for estrogenicity, androgenicity, and aromatase activity in vitro. Toxicol Appl Pharmacol 2002;179(1):1–12. [PubMed: 11884232]

Beere HM. Death versus survival: functional interaction between the apoptotic and stress-inducible heat shock protein pathways. J Clin Invest 2005;115(10):2633–2639. [PubMed: 16200196]

Blonska M, Shambharkar PB, Kobayashi M, Zhang D, Sakurai H, Su B, Lin X. TAK1 is recruited to the Tumor Necrosis Factor-α (TNF-α) Receptor 1 Complex in a Receptor-interacting Protein (RIP)-dependent Manner and cooperates with MEKK3 leading to NF-κB activation. J Biol Chem 2005;280 (52):43056–43063. [PubMed: 16260783]

Bloomquist JR, Barlow RL, Gillette JSW, Li Kirby ML. Selective effects of insecticides on nigrostriatal dopaminergic nerve pathways. Neurotoxicology 2002;23(4–5):537–544. [PubMed: 12428726]

Cai B, Chang SH, Becker EBE, Bonni A, Xia Z. p38 MAP Kinase mediates apoptosis through phosphorylation of Bim_{EL} at Ser-65. J Biol Chem 2006;281(35):25215–25222. [PubMed: 16818494]

Caroline C. Insecticide fact sheet, Chlorpyrifos. Part 1 Toxicology. J Pest Reform 1994;14:15–20.

Caserta TM, Smith AN, Gultice AD, Reedy MA, Brown TL. Q-VD-OPh, a broad spectrum caspase inhibitor with potent antiapoptotic properties. Apoptosis 2003;8(4):345–52. [PubMed: 12815277]

Caughlan A, Newhouse K, Namgung U, Xia Z. Chlorpyrifos induces apoptosis in rat cortical neurons that is regulated by a balance between p38 and ERK/JNK MAP kinases. Toxicol Sci 2004;78:125–134. [PubMed: 14691213]

Chang L, Karin M. Mammalian MAP kinase signalling cascades. Nature 2001;410:37–40. [PubMed: 11242034]

Crumpton TL, Seidler FJ, Slotkin TA. Developmental neurotoxicity of chlorpyrifos in vivo and in vitro: effects on nuclear transcription factors involved in cell replication and differentiation. Brain Res 2000;857:87–98. [PubMed: 10700556]

Chen G, Goeddel DV. TNF-R1 Signaling: A Beautiful Pathway. Science 2002;296:1634–1635. [PubMed: 12040173]

Dam K, Seidler FJ, Slotkin TA. Chlorpyrifos releases norepinephrine from adult and neonatal rat brain synaptosomes. Brain Res Dev Brain Res 1999;118(1–2):129–33.

Devin A, Cook A, Lin Y, Rodriguez Y, Kelliher M, Liu Z. The distinct roles of TRAF2 and RIP in IKK activation by TNF-R1: TRAF2 recruits IKK to TNF-R1 while RIP mediates IKK activation. Immunity 2000;12(4):419–29. [PubMed: 10795740]

Eskenazi B, Marks AR, Bradman A, Harley K, Barr DB, Johnson C, Morga N, Jewell NP. Organophosphate Pesticide Exposure and Neurodevelopment in Young Mexican-American Children. Environ Health Perspect 2007;115(5):792–798. [PubMed: 17520070]

Fenske RA, Kedan G, Lu C, Fisker-Andersen JA, Curl CL. Assessment of organophosphorous pesticide exposures in the diets of preschool children in Washington State. J Expo Anal Environ Epidemiol 2002a;12(1):21–8. [PubMed: 11859430]

Fenske RA, Lu C, Barr D, Needham L. Children's exposure to chlorpyrifos and parathion in an agricultural community in central Washington State. Environ Health Perspect 2002b;110(5):549–553. [PubMed: 12003762]

Garcia SJ, Seidler FJ, Slotkin TA. Developmental neurotoxicity eli cited by prenatal or postnatal chlorpyrifos exposure: effects on nonspecific proteins indicate changing vulnerabilities. Environ Health Perspect 2003;111:297–303. [PubMed: 12611658]

Giordano G, Afsharinejad Z, Guizzetti M, Vitalone A, Kavanagh TJ, Costa LG. Organophosphorus insecticides chlorpyrifos and diazinon and oxidative stress in neuronal cells in a genetic model of glutathione deficiency. Toxicol Appl Pharmacol 2007;219(2–3):181–9. [PubMed: 17084875]

Gordon CJ, Rowsey PJ. Are circulating cytokines interleukin-6 and tumor necrosis factor alpha involved in chlorpyrifos-induced fever? Toxicology 1999;134(1):9–17. [PubMed: 10413184]

Guo Y, Hendricks AG, Overstreet JW, Dieter J, Stewart D, Tarantal AF, Laughlin L, Lasley BL. Endocrine biomarkers of early fetal loss in cynomolgus macaques (*Macaca fascicularis*) following exposure to dioxin. Biol Reprod 1999;60:707–13. [PubMed: 10026120]

Houston A, O'Connell J. The Fas signalling pathway and its role in the pathogenesis of cancer. Current Opin Pharmacol 2004;4(4):321–326.

Itoh N, Yonehara S, Ishii A, Yonehara M, Mizushima S, Sameshima M, Hase A, Seto Y, Nagata S. The polypeptide encoded by the cDNA for human cell surface antigen Fas can mediate apoptosis. Cell 1991;66(2):233–43. [PubMed: 1713127]

Ivey MC. Chlorpyrifos and 3,5,6,-trichloro-2-pyridinol: residues in the body tissues of cattle wearing chlorpyrifos-impregnated plastic ear tags. J Econ Entomol 1979;72(6):909–11. [PubMed: 93609]

Ivey MC, Palmer JS. Chlorpyrifos and 3,5,6-trichloro-2-pyridinol: residues in body tissues of swine treated with chlorpyrifos for hog louse and itch mite control. J Econ Entomol 1979;2(6):837–8. [PubMed: 93608]

Ivey MC, Palmer JS. Chlorpyrifos and 3,5,6-trichloro-2-pyridinol: residues in the body tissues of sheep treated with chlorpyrifos for sheep ked control. J Econ Entomol 1981;74(2):136–7. [PubMed: 6172455]

Karanth S, Liu J, Mirajkar N, Pope C. Effects of acute chlorpyrifos exposure on in vivo acetylcholine accumulation in rat striatum. Toxicol Appl Pharmacol 2006;216(1):150–156. [PubMed: 16777161]

Kreuz S, Siegmund D, Rumpf JJ, Samel D, Leverkus M, Janssen O, Hacker G, Dittrich-Breiholz O, Kracht M, Scheurich P, Wajant H. NFκB activation by Fas is mediated through FADD, caspase-8, and RIP and is inhibited by FLIP. J Cell Biol 2004;166 (3):369–380. [PubMed: 15289496]

Li L, Shou Y, Borowitz JL, Isom GE. Reactive Oxygen Species Mediate Pyridostigmine-Induced Neuronal Apoptosis. Involvement of Muscarinic and NMDA Receptors Toxicol Appl Pharmacol 2001;177(1):17–25.

Li X, Minden A. PAK4 Functions in Tumor Necrosis Factor (TNF) α-induced Survival Pathways by Facilitating TRADD Binding to the TNF Receptor. J Biol Chem 2005;280(50):41192–41200. [PubMed: 16227624]

Lu C, Fenske RA, Simcox NJ, Kalman D. Pesticide exposure of children in an agricultural community: evidence of household proximity to farmland and take home exposure pathways. Environ Res 2000;84(3):290–302. [PubMed: 11097803]

Mattsson JL, Maurissen JPJ, Nolan RJ, Brzak KA. Lack of Differential Sensitivity to Cholinesterase Inhibition in Fetuses and Neonates Compared to Dams Treated Perinatally with Chlorpyrifos. Toxicol Sci 2000;53:438–446. [PubMed: 10696792]

Mansouri A, Ridgway LD, Korapati AL, Zhang Q. Sustained activation of JNK/p38 MAPK pathways in response to cisplatin leads to Fas Ligand induction and cell death in ovarian carcinoma cells. J Biol Chem 2003;278(21):19245–19256. [PubMed: 12637505]

Moser VC. Dose–response and time-course of neurobehavioral changes following oral chlorpyrifos in rats of different ages. Neurotoxicol Teratol 2000;22(5):713–23. [PubMed: 11106864]

Myllynen P, Pasanen M, Pelkonen O. Human placenta: a human organ for developmental toxicology research and biomonitoring. Placenta 2005;26:361–371. [PubMed: 15850640]

Naarala J, Tervo P, Loikkanen J, Savolainen K. Cholinergic-induced production of reactive oxygen species in human neuroblastoma cells. Life Sci 1997;60(21):1905–14. [PubMed: 9155001]

Nakadai A, Li Q, Kawada T. Chlorpyrifos induces apoptosis in human monocyte cell line U937. Toxicology 2006;224(3):202–209. [PubMed: 16787693]

Namgung U, Xia Z. Arsenite-induced apoptosis in cortical neurons is mediated by c-Jun N-terminal protein kinase 3 and p38 mitogen-activated protein kinase. J Neurosci 2000;20(17):6442–6451. [PubMed: 10964950]

Nativelle-Serpentini C, Richard S, Seralini GE, Sourdaine P. Aromatase activity modulation by lindane and bisphenol-A in human placental JEG-3 and transfected kidney E293 cells. Toxicol In Vitro 2003;17(4):413–22. [PubMed: 12849724]

Nemoto S, Xiang J, Huang S, Lin A. Induction of Apoptosis by SB202190 through Inhibition of p38β Mitogen-activated Protein Kinase. J Biol Chem 1998;273(26):16415–16420. [PubMed: 9632706]

Oldenburg O, Qin Q, Sharma AR, Cohen MV, Downey JM, Benoit JN. Acetylcholine leads to free radical production dependent on K(ATP) channels, G(i) proteins, phosphatidylinositol 3-kinase and tyrosine kinase. Cardiovasc Res 2002;55(3):544–52. [PubMed: 12160951]

Perera FP, Rauh V, Tsai WY, Kinney P, Camann D, Barr D, Bernert T, Garkinkel R, Tu YH, Diaz D, Dietrich J, Whatt RM. Effects of transplacental exposure to environmental pollutants on birth outcomes in a multiethnic population. Environ Health Perspect 2003;111(2):201–205. [PubMed: 12573906]

Perera FP, Rauh V, Whyatt RM, Tang D, Tsai WY, Bernert JT, Tu YH, Andrews H, Barr DB, Camman DE, Diaz D, Dietrich J, Reyes A, Kinney PL. A summary of recent findings on birth outcomes and developmental effects of prenatal ETS, PAH, and pesticide exposures. Neurotoxicology 2005;26(4): 573–87. [PubMed: 16112323]

Qian D, Seidler FJ, Slotkin TA. Developmental neurotoxicity of chlorpyrifos modeled in vitro: comparative effects of metabolites and other cholinesterase inhibitors on DNA synthesis in PC-12 and C-6 glioma cells. Environ Health Perspect 2001;109:909–13. [PubMed: 11673119]

Qiao D, Seidler FJ, Slotkin TA. Oxidative mechanisms contributing to the developmental neurotoxicity of nicotine and chlorpyrifos. Toxicol Appl Pharmacol 2005;206(1):17–26. [PubMed: 15963341]

Rauh VA, Garfinkel R, Perera FP, Andrews HF, Hoepner L, Barr DB, Whitehead R, Tang D, Whatt RW. Impact of prenatal chlorpyrifos exposure on neurodevelopment in the first three years of life among inner-city children. Pediatrics 2006;118:1845–1859.

Ricceri L, Venerosi A, Capone F, Cometa MF, Lorenzini P, Fortuna S, Calamandrei G. Developmental Neurotoxicity of Organophosphorous Pesticides: Fetal and Neonatal Exposure to Chlorpyrifos Alters Sex-Specific Behaviors at Adulthood in Mice. Toxicol Sci 2006;93(1):105–13. [PubMed: 16760416]

Rowsey PJ, Gordon CJ. Tumor necrosis factor is involved in chlorpyrifos-induced changes in core temperature in the female rat. Toxicol Lett 1999;109(1–2):51–9. [PubMed: 10514030]

Sagik SK, Tolbert PE, Altshui LM, Korrick SA. Organochlorine exposures during pregnancy and infant size at birth. Epidemiology 2007;18(1):120–9. [PubMed: 17179760]

Sastry BV. Human placental cholinergic system. Biochem Pharmacol 1997;53(11):1577–86. [PubMed: 9264309]

Slotkin TA, Oliver CA, Seidler FJ. Critical periods for the role of oxidative stress in the developmental neurotoxicity of chlorpyrifos and terbutaline, alone or in combination. Brain Res Dev Brain Res 2005;157(2):172–80.

Slotkin TA, Seidler FJ. Prenatal chlorpyrifos exposure elicits presynaptic serotonergic and dopaminergic hyperactivity at adolescence: critical periods for regional and sex-selective effects. Reprod Toxicol 2007;23(3):421–7. [PubMed: 17267174]

Souza MS, Magnarelli de Potas G, Pechén de D'Angelo AM. Organophosphorous and organochlorine pesticides affect human placental phosphoinositides metabolism and PI-4 kinase activity. J Biochem Mol Toxicol 2004;18(1):30–6. [PubMed: 14994277]

Strasser A, O'Connor L, Dixit VM. Apoptosis signaling. Ann Rev Biochemistry 2000;69:217–245.

Suzuki Y, Aoki K, Saito H, Umeda M, Nitta H, Baron R, Ohya K. A tumor necrosis factor-α antagonist inhibits inflammatory bone resorption induced by *Prophyromonas gingivalis* infection in mice. J Periodont Res 2006;41:81–91. [PubMed: 16499710]

Tanel A, Averill-Bates DA. P38 and ERK mitogen-activated protein kinases mediate acrolein-induced apoptosis in Chinese hamster ovary cells. Cell Signal 2007;19(5):968–977. [PubMed: 17196791]

Thrasher JD, Heuser G, Broughton A. Immunological abnormalities in humans chronically exposed to chlorpyrifos. Arch Environ Health 2002;57(3):181–7. [PubMed: 12507170]

Tuzmen N, Candan N, Kaya E, Demiryas N. Biochemical effects of chlorpyrifos and deltamethrin on altered antioxidative defense mechanisms and lipid peroxidation in rat liver. Cell Biochem Funct. 2007in press

Whyatt RM, Rauh V, Barr DB, Camann DE, Andrews HF, Garfinkel R, Hoepner LA, Diaz D, Dietrich J, Reyes A, Tang D, Kinney PL, Perera FP. Prenatal insecticide exposures and birth weight and length among an urban minority cohort. Environ Health Perspect 2004;112:1125–1132. [PubMed: 15238288]

Whyatt RM, Garfinkel R, Hoepner LA, Holmes D, Borjas M, Williams MK, Reyes A, Rauh V, Perera FP, Camann DE. Within- and Between-Home Variability in Indoor-Air Insecticide Levels during

Pregnancy among an Inner-City Cohort from New York City. Environ Health Perspect 2007;115(3): 383–389. [PubMed: 17431487]

Yang L, Sugama S, Mischak RP, Kiaei M, Bizat N, Brouillet E, Joh TH, Beal MF. A novel systemically active caspase inhibitor attenuates the toxicities of MPTP, malonate and 3NP in vivo. Neurobiol Dis 2004;17:250–259. [PubMed: 15474362]

Zhou Y, Wang Q, Evers BM, Chung DH. Oxidative stress-induced intestinal epithelial cell apoptosis is mediated by p38 MAPK Biochem. Biophys Res Commun 2006;350(4):860–5.

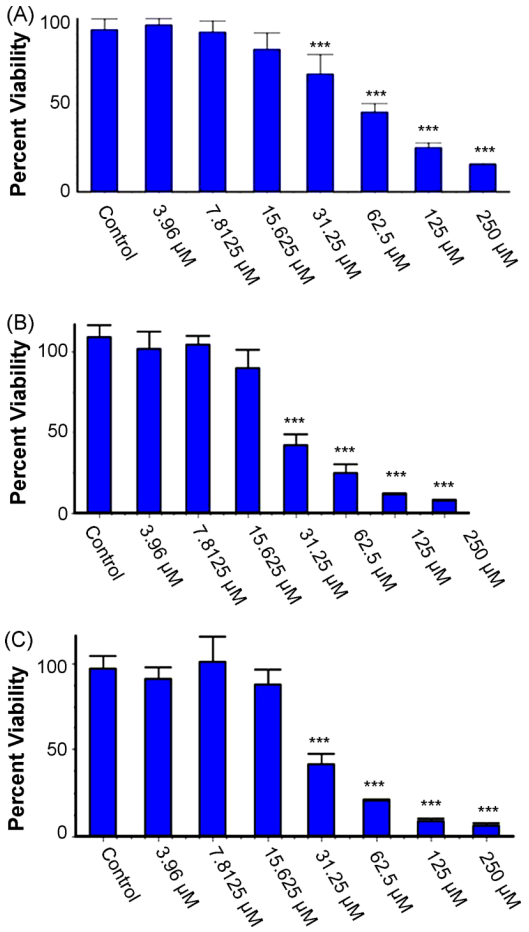

Figure 1. The effects of Chlorpyrifos (CPF) on JAR viability

JAR cells were incubated with various concentrations ranging from approximately 3μM–250μM for 24, 48 and 72 hours. Panel A represents the toxic effect of CPF at 24 hours, Panel B is 48 hours and Panel C is 72 hours. Data is representative of at least three independent experiments. Statistical analysis was performed using one way ANOVA. The asterisk"***" denotes that treatment is significantly different from the control ($p<0.001$).

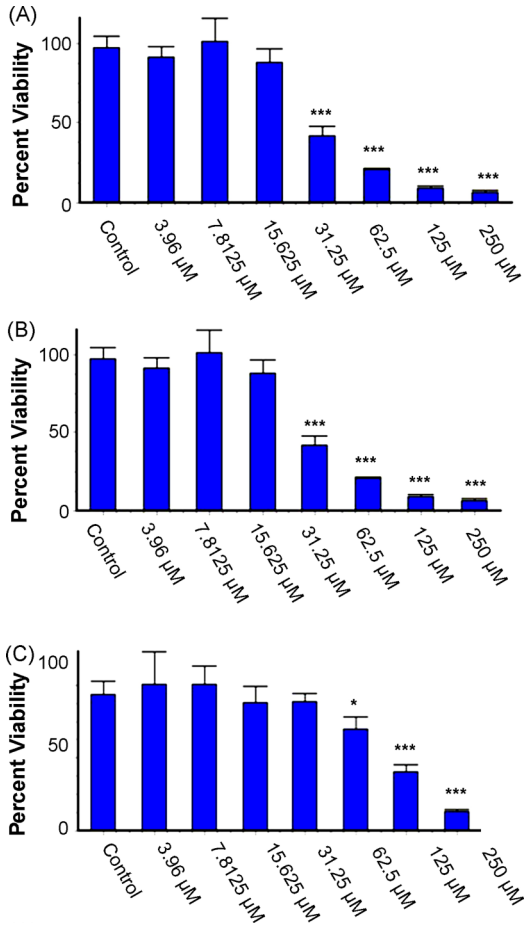

Figure 2. The effects of Chlorpyrifos-oxon (CPO) on JAR viability

JAR cells were incubated with various concentrations ranging from approximately 3μM–250μM for 24, 48 and 72 hours. Panel A represents the toxic effect of CPO at 24 hours, Panel B is 48 hours and Panel C is 72 hours. Data is representative of at least three independent experiments. Statistical analysis was performed using one way ANOVA. The asterisk"***" denotes that treatment is significantly different from the control ($p<0.001$).

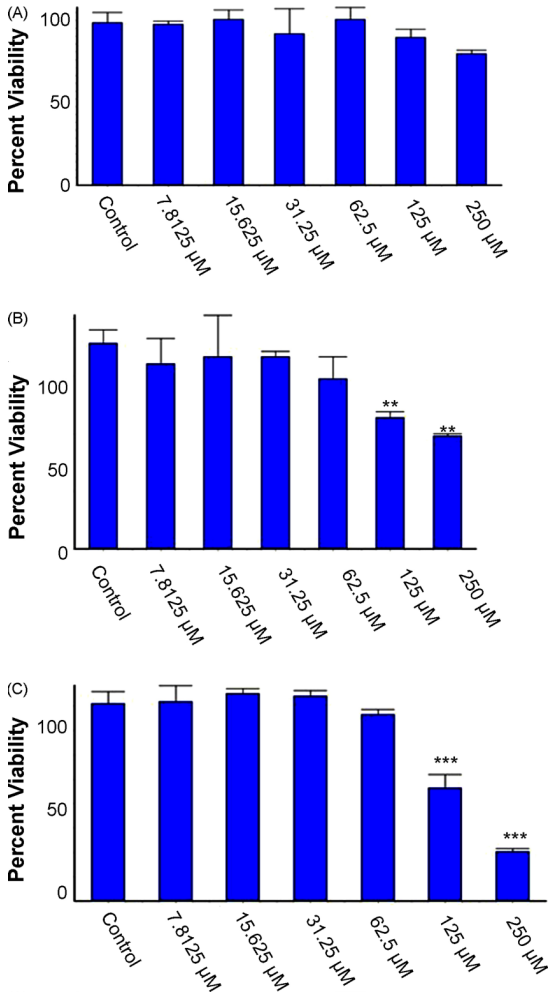

Figure 3. The Effects of Chlorpyrifos metabolite 3,5,6-trichloro-2-pyridinol (TCP) on JAR Viability

JAR cells were incubated with various concentrations ranging from approximately 3μM–250μM for 24, 48 and 72 hours. Panel A represents the toxic effect of TCP at 24 hours, Panel B is 48 hours and Panel C is 72 hours. Data is representative of at least three independent experiments. Statistical analysis was performed using one way ANOVA. The asterisk"***" denotes that treatment is significantly different from the control ($p<0.001$).

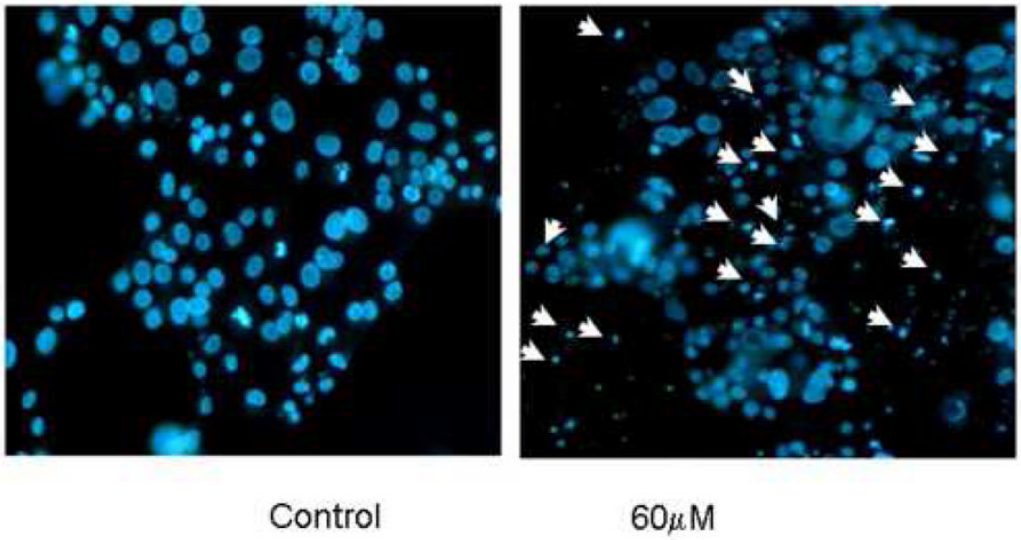

Figure 4. The Effects of Chlorpyrifos on Nuclear Morphology

Nuclear morphology was determined using Hoechst stain. JAR cells were incubated with 60μM Chlorpyrifos or drug vehicle for 24 hours. The white arrows denote cells with fragmented and/or condensed nuclei. Images were acquired under 20X magnification.

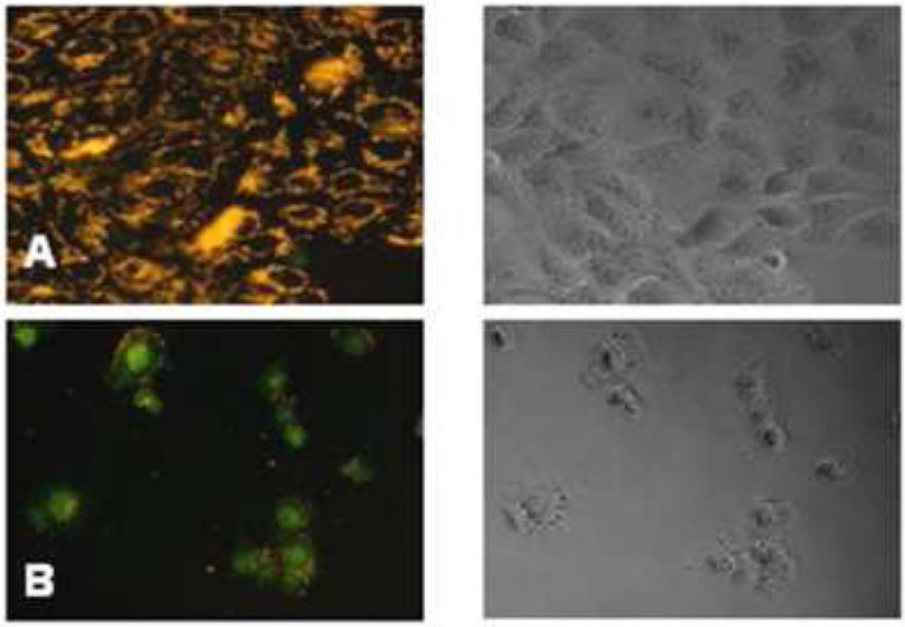

Figure 5. The Effects of Chlorpyrifos on of Mitochondrial Potential

JAR cells were incubated with 60uM Chlorpyrifos or drug vehicle for 24 hours. Actively respiring (healthy mitochondria) convert the green monomeric form of the dye to the aggregate form which are associated a color change to red-orange. Damaged mitochondria fail to convert the dye to its "red" aggregate form. Panel A represents JAR cells incubated with the drug vehicle for 24 hours whereas Panel B represents JAR cells exposed to 60uM Chlorpyrifos. The right panels are the same cells observed using phase-contrast microscopy. Images were acquired under 20X magnification.

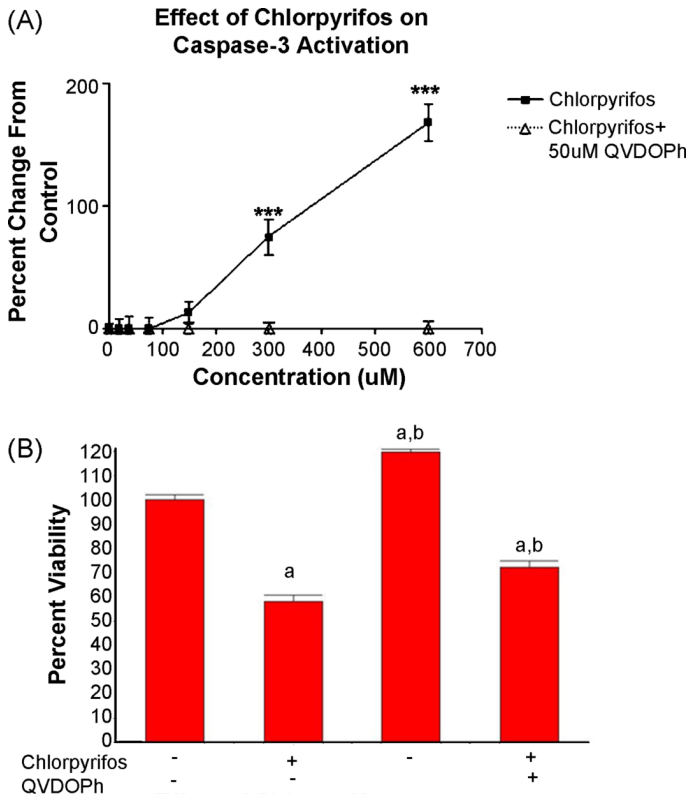

Figure 6. The Effects of Pan-caspase inhibitor Q-VD-OPh on CPF-induced cytotoxicity and Activation of Caspase 3/7

Figure 6A represents the effects of various concentrations of CPF on Caspase 3 activity. JAR cells were exposed to various concentrations CPF (18–600 μM) for four hours. CPF caused a dose-dependent increase in caspase3/7. Only concentrations greater than 150μM CPF caused significant differences (*** denotes $p<0.0001$) in enzyme activity relative to control. Figure 6B represents the effect of 50μM Q-VD-O-Ph on CPF-induced cytotoxicity in JAR cells. Q-VD-O-Ph partially reverses CPF-induced toxicity in JAR cells were treated with 60 μM of CPF, 50μM of Pan-caspase inhibitor Q-VD-OPh, and 60μM of CPF + 50 μM of Pan-caspase inhibitor QVDOPh over a 24 hour period. Cellular viability was assessed by Alamar Blue assay. Percent viability is the percentage of cells dying versus relative control. The “a” denotes treatment significantly different from control ($p< 0.001$). The “b” denotes treatment significantly different from control CPF ($p<0.001$). All data is representative of three (3) independent experiments. Data is represented as the mean percent change from control ± SEM.

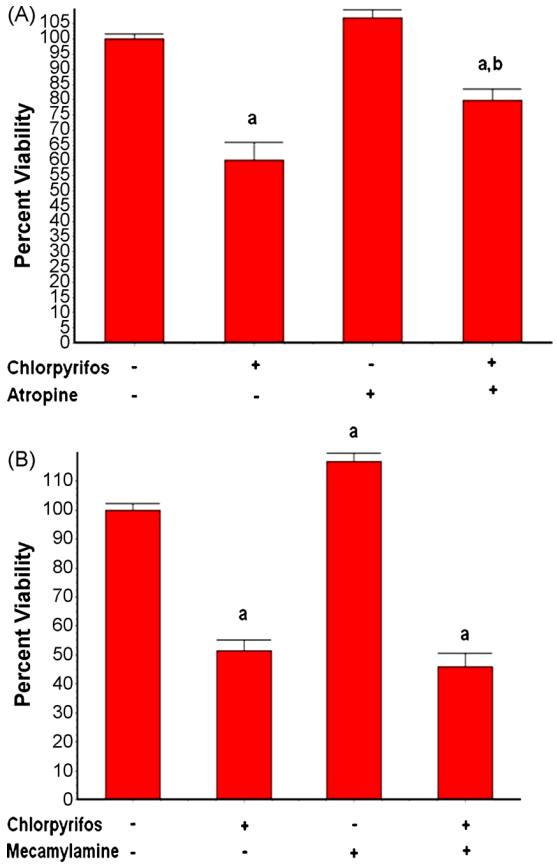

Figure 7. CPF induced toxicity in the presence and absence of cholinergic antagonists

FIG 7A. JAR were treated with 60 μM of CPF, 10 μM of Atropine, and 60 μM CPF + 10 μM of Atropine over a 24 hour period. FIG 7B. JAR were treated with 60 μM CPF, 10 μM of Mecamylamine, and 60 μM CPF + 100 μM of Mecamylamine. Cellular viability was assessed by Alamar Blue assay. Percent viability is the percentage of cells dying versus relative control. The "a" denotes treatment significantly different from control ($p < 0.001$). The "b" denotes treatment significantly different from control CPF ($p<0.001$). Data is represented as the mean ± SEM. All data is representative of three (3) independent experiments.

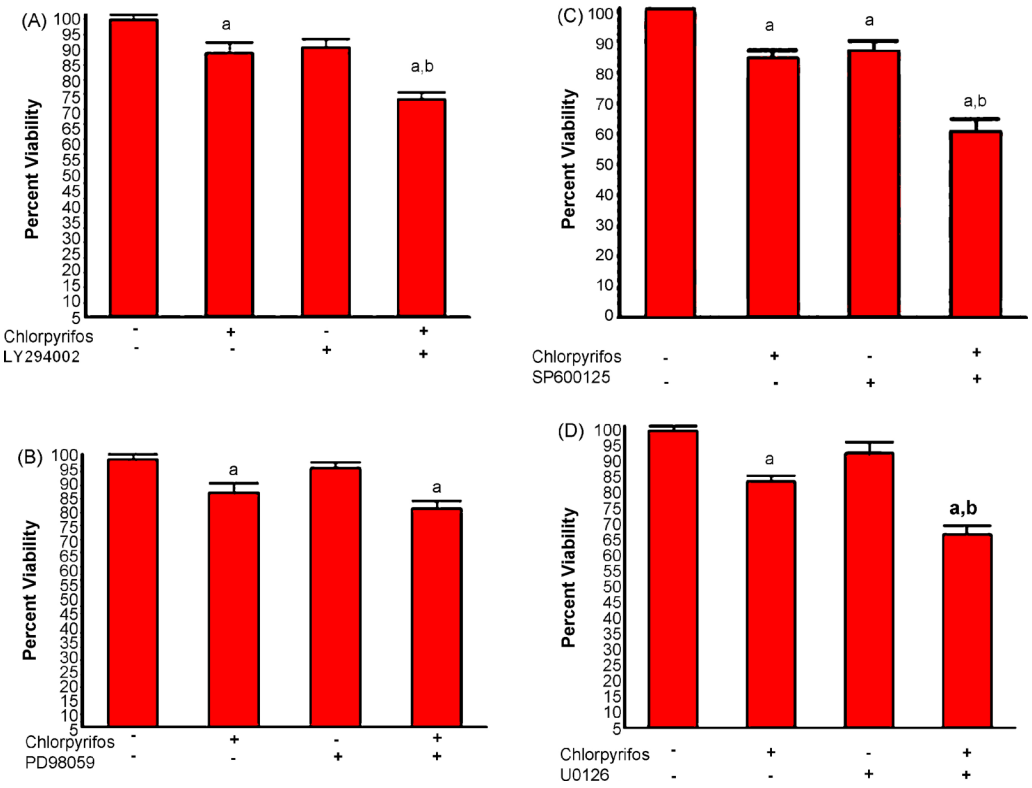

Figure 8. The Effects of Signal Transduction Inhibitors on Chlorpyrifos-induced toxicity

In panel A, JAR cells were exposed to DMSO in media (drug vehicle) or with 60μM CPF, 20μM LY294002, and a combination of 60 μM CPF with 20 μM LY294002. In panel B, JAR cells were exposed to DMSO in media (drug vehicle) or treated 60 μM CPF, 20 μM PD98059 and 60 μM CPF + 20 μM of PD98059. In panel C, JAR cells were exposed to DMSO in media (drug vehicle) or treated with 60 μM CPF, 10 μM SP600125, and 60 μM CPF + 10 μM of SP600125. In panel D, JAR cells were exposed to 60 μM of CPF, 10 μM of U0126, and 60 μM of CPF + 10μM of U0126. All drugs were incubated for 12 hours. Cellular viability was assessed by Alamar Blue assay. Percent viability is expressed as the percentage of cells dying versus relative control. Data is expressed as the mean ± SEM. The data presented in each graph is representative of at least three independent experiments. Statistical analysis was performed using one way ANOVA. The “a” denotes treatment significantly different from control ($p < 0.001$). The “b” denotes treatment significantly differently CPF ($p < 0.001$).

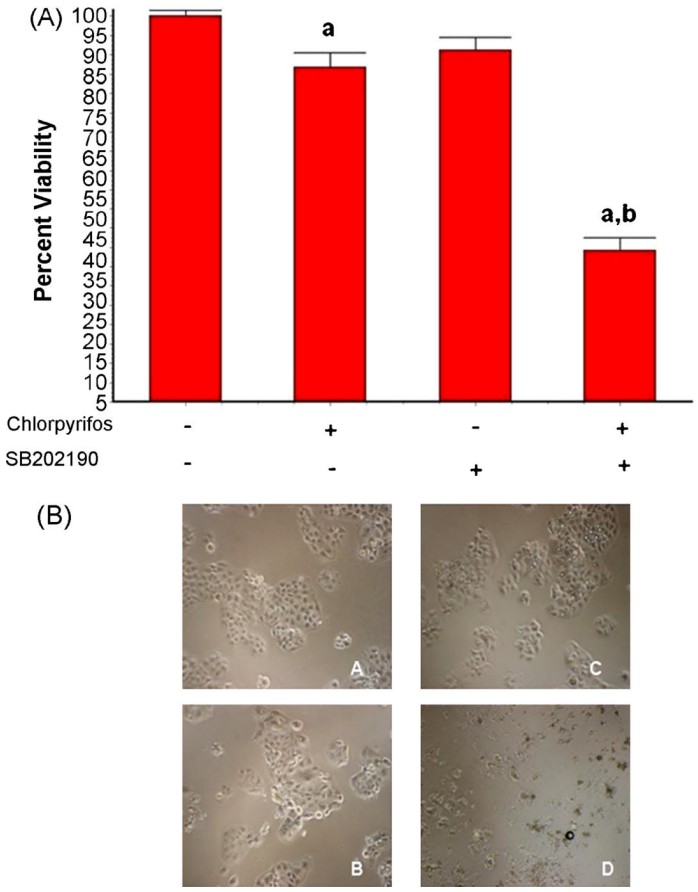

Figure 9. The p38 inhibitor SB202190 induces cellular death in human placental (JAR) cells

In Figure 7A the JAR cells were exposed to DMSO in media (drug vehicle). JAR were treated with concentration of 60 μM of CPF, 10 μM of SB202190, and CPF + SB202190 over a 12 hour period. Cellular viability was assessed by Alamar Blue assay. Percent viability is the percentage of cells dying versus relative control. The "a" denotes treatment significantly different from control ($p < 0.001$). The "b" denotes treatment significantly different from CPF ($p < 0.001$). Data is represented as the mean ± SEM. In figure 7B illustrates the cells morphology of the cells exposed to CPF and or SB202190. Cells were observed using a Nikon inverted microscope. Panel A represents Control, Panel B represents JAR treated with 60 μM CPF, Panel C represents JAR treated with 10 uM SB202190 and Panel D represents JAR treated with CPF + SB202190. All Panels (A – thru D) were analyzed following 12 hour exposure period. All data is representative of three (3) independent experiments.

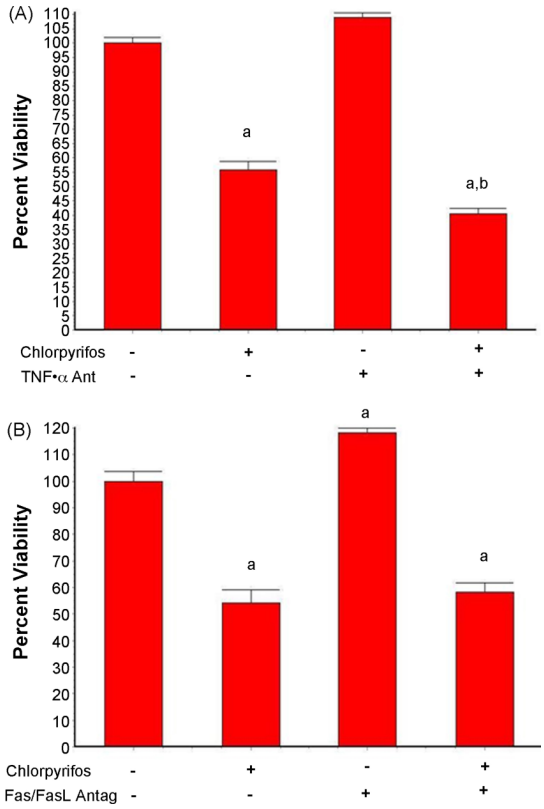

Figure 10. The Effects of TNF-α Receptor Antagonists and FAS and FAS Ligand Antagonists on CPF Induced Toxicity in JAR Cells

Fig 10A JAR were treated with 60 μM CPF, 10μM of TNF-α Receptor Antagonists, and 60μM CPF + 10μM TNF-α Receptor Antagonists over a 24 hour period. Cellular viability was assessed by Alamar Blue. Percent viability is the percentage of cells dying versus relative control. The “a” denotes treatment significantly different from control ($p < 0.001$). The “b” denotes treatment significantly different from control CPF ($p<0.001$). Fig 10B JAR were treated with 60 uM of CPF, 1 mg/ml of Fas/Fas Ligand Antagonists, and 60μM CPF + 1 mg/ml Fas/Fas Ligand Antagonist over a 24 hour period. Cellular viability was assessed by Alamar Blue. Percent viability is the percentage of cells dying versus relative control. The “a” denotes treatment significantly different from control ($p < 0.001$). The “b” denotes treatment significantly different from control CPF ($p<0.001$).

TABLE 1
The Effects of Staurosporine and Q-VD-OPh on Caspase 3/7 Activity in JAR Cells

JAR cells were incubated with 50 μMQ-VD-OPh and/or 10μM staurosporine for 4 hours. Caspase activity is expressed as the mean percent change +/− standard error of the mean over caspase activity in cells treated with DMSO-drug vehicle. Data is representative of at least three independent experiments.

Compound	%Change From Control ± SEM
Staurosporine (10μM)	182± 30.9
Q-VD-O-Ph (50μM)	−54.7± 6.7
Q-VD-O-Ph (50μM) With Staurosporine (10μM)	−51.1± 19.7

TABLE 2
The Effects of CPF on Gene Expression in JAR Cells

JAR cells were incubated with 60μM chlorpyrifos (CPF) or drug vehicle for 24 hours. Fold change represents the ratio of the mean gene expression of cells treated with CPF to the mean gene expression of cells treated with DMSO drug vehicle. All data is representative of at least four (4) independent experiments

Gene	Gene Accession Number	Fold Induction or Reduction	Statistics
BCL2 (B-cell CLL/lymphoma 2)	NM_000633	−1.53	p<0.05
CDKN2A (Cyclin-dependent kinase inhibitor)	NM_000077	−1.88	p<0.001
FAS (TNF receptor superfamily, member 6)	NM_000043	15.89	p<0.001
ITGA4 (Antigen CD49D)	NM_000885	5.62	p<0.001
ITGB1 (Fibronectin receptor)	NM_002221	3.28	p<0.01
MTA2 (Metastasis associated 1 family, member 2)	NM_004739	−3.16	p<0.01
TEK (TEK tyrosine kinase, endothelial)	NM_000459	−2.20	p<0.01
TNF (Tumor necrosis factor)	NM_000594	11.84	p<0.01
TWIST1 (Twist homolog 1)	NM_000474	−2.08	p<0.01